Geomechanics and Engineering, *Vol. 36, No. 5 (2024) 417-426*
https://doi.org/10.12989/gae.2024.36.5.417

Effect of the support pressure modes on face stability during shield tunneling

Dalong Jin[1,2], Yinzun Yang*[1,2], Rui Zhang[3], Dajun Yuan[1,2] and Kang Zhang[3]

[1]*Key Laboratory of Urban Underground Engineering of Ministry of Education, Beijing Jiaotong University, Beijing, China*
[2]*School of Civil Engineering, Beijing Jiaotong University, Beijing 100044, China*
[3]*Jinan Rail Transit Group Co, Ltd, Jinan 250000, China*

(*Received January 30, 2022, Revised October 6, 2023, Accepted February 5, 2024*)

Abstract. Shield tunneling method is widely used to build tunnels in complex geological environment. Stability control of tunnel face is the key to the safety of projects. To improve the excavation efficiency or perform equipment maintenance, the excavation chamber sometimes is not fully filled with support medium, which can reduce the load and increase tunneling speed while easily lead to ground collapse. Due to the high risk of the face failure under non-fully support mode, the tunnel face stability should be carefully evaluated. Whether compressive air is required for compensation and how much air pressure should be provided need to be determined accurately. Based on the upper bound theorem of limit analysis, a non-fully support rotational failure model is developed in this study. The failure mechanism of the model is verified by numerical simulation. It shows that increasing the density of supporting medium could significantly improve the stability of tunnel face while the increase of tunnel diameter would be unfavorable for the face stability. The critical support ratio is used to evaluate the face failure under the non-fully support mode, which could be an important index to determine whether the specific unsupported height could be allowed during shield tunneling. To avoid of face failure under the non-fully support mode, several charts are provided for the assessment of compressed air pressure, which could help engineers to determine the required air pressure for face stability.

Keywords: pressure gradient; shield tunnelling; support mode; support ratio; tunnel face stability

1. Introduction

Shield tunneling method is widely used to build tunnels all over the world. During shield tunneling, face stability is the key for engineering safety (Yuan *et al.* 2017, Li *et al.* 2019). The external soil and water pressure are balanced with support pressures in excavation chamber of the shield machine. If the support pressure is not enough, soil could move into the excavation chamber rapidly, resulting ground collapse accidents (Jin *et al*. 2021, Lu *et al.* 2021, Wang *et al.* 2021). During the past few years, the failure mechanism of tunnel face has been studied by many scholars through theoretical analysis (Subrin and Wong 2002, Wang *et al.* 2013, Tang *et al.* 2014, Zou *et al.* 2019), model tests (Juneja *et al.* 2010, Liu *et al*. 2018, Liu *et al.* 2021) and numerical simulation (Paternesi *et al.* 2017, Zhang *et al.* 2011). Yang and Huang (2011) proposed a formula of the height and width of failure block.

The conclusion indicates that the half width of the top and bottom of failure block increases with the increase of values of material constants A. Mollon *et al.* (2011) proposed three-dimensional rotational failure model. Both the upper solution and lower solution of critical support pressures were provided in his study. Perazzelli *et al*. (2014) derived a closed-form solution for the limit support pressure of tunnel face under seepage flow conditions. Pan and Dias (2016) studied the influence of groundwater level and anisotropic permeability on upper limit solution of critical support pressure by combining kinematic method and FLAC^{3D}. On the basis of original Protodyakonov's arch model, Ji *et al.* (2018) discussed the influence of tunnel diameter and cover depth on support pressure of pipe jacking tunnel. The influence of three-dimensional arch effect was considered in his study and the calculation results were verified by numerical simulations.

Sterpi and Cividini (2004) studied the stability of tunnel face in strain softening frictional medium through model tests. Kirsch (2010) carried out some model tests in dry sandy ground, and studied the critical support pressure of the tunnel face. The results show that the initial density of sand has important influence on the formation and development of collapse mechanism. Through a series of model tests with different soil cover, Chen *et al*. (2013) divided the failure of tunnel face into two stages: local failure and global failure. Meanwhile, the evolution process of soil arch was discussed. Chen *et al*. (2018) studied the failure of tunnel face caused by steady seepage in saturated sandy silty soil through a series of centrifuge tests, and also explored the change of effective support pressure during the failure process of tunnel face.

Eberhardt (2001) explored the spatial and temporal stress paths in tunnelling through numerical simulation. Based on kinematical element method, Qarmout *et al*. (2019) proposed a numerical model to obtain the minimum support pressure for tunneling in dry frictional soil.

*Corresponding author, Ph.D.
E-mail: yangyinzun2021@163.com

ISSN: 2005-307X (Print), 2092-6219 (Online)

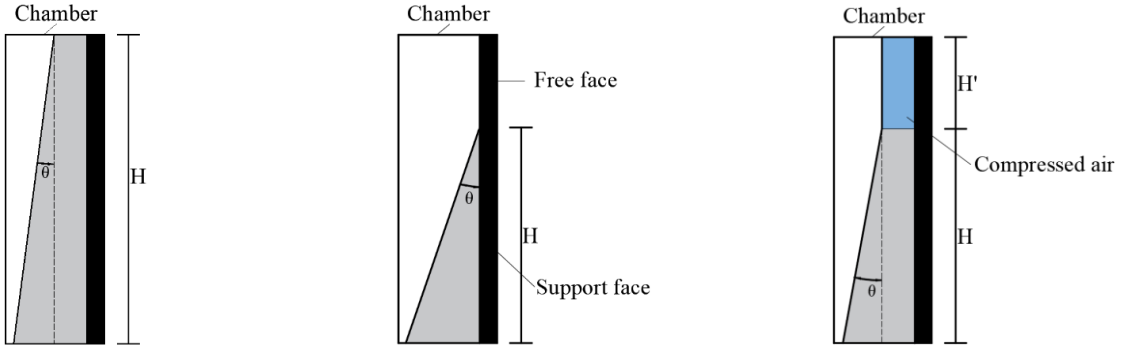

Fig. 1 Support pressure modes in excavation chamber: (a)fully support mode and (b) non-fully support mode (black: tunnel face, grey: supporting medium pressure, blue: compressed air pressure)

In engineering practices, the excavation chamber is usually not full of supporting medium and the support pressure cannot fully act on the entire tunnel face. However, all of the previous studies are aimed at the analysis of face stability for the cases of uniformly and fully distributed support pressure in excavation chamber, which could overestimate the stability of tunnel face. The non-fully support pressure usually comes from two situations: expected and unexpected cases. In the expected cases, the incomplete support pressure could be selected to improve the tunneling efficiency or used for equipment maintenance (Zhu *et al.* 2006. Tian *et al.* 2019). The thrust and torque of the shield machine with non-fully support medium in the excavation chamber is much smaller than that of fully support chamber, which can greatly improve the advance rate of the shield machine. Due to the space requirement, the inspect and replacement of the cutters usually also need to be conducted under non-fully support mode. In the unexpected cases, due to the poor liquidity of the soil muck, the excavation chamber also cannot be filled with soil muck, resulting a non-fully support pressure on the tunnel face. The non-fully support modes could significantly reduce the face stability and ground collapse may be easily caused. Hence, sometimes, compressive air pressures are need to be provided to keep the face stability under non-fully support modes.

This study focuses on the face stability of shield tunneling under different support modes on the basis of the kinematical approach of limit analysis. A non-fully support model is developed to evaluate the face stability based on the rotational failure mechanism proposed by Mollon (2011). In order to validate the presented method, the critical support pressure obtained are compared with numerical simulations. The critical support ratio for both the cases of global failure and local failure are discussed. Several charts are provided for the assessment of compressed air pressure, which could help engineers to determine the required air pressure for face stability.

2. Three-dimensional rotational model

2.1 Support modes analysis

As shown in Fig. 1, the support pressure distribution could be summarized as two modes: (a) Fully support mode, namely, the excavation chamber is completely filled with support medium, such as soil muck and bentonite slurry. This is also the most common mode when tunneling by shield machines. The support pressure is usually distributed as trapezoidal because of soil gravity; (b) Non-fully support mode: In this case, the support medium cannot completely fill the excavation chamber and leaves some gaps in the upper part. Sometimes, to avoid of face failure, the upper gap of the excavation chamber is filled with compressed air to ensure the face stability under poor geology conditions (Zhu *et al*. 2020, Zhang *et al.* 2020, Nagel and Meschke 2010).

The typical schematic diagram of the non-fully support mode is shown in Fig. 2. The part of tunnel face supported by supporting medium is called support face while the upper part is the free face. The diameter of shield tunnel is D, the cover depth is C and H is the height of support face. The support ratio is defined as H/D, l.e. the ratio of support face height to tunnel diameter. σ_s is the critical support pressure of supporting medium acting on the support face. σ_A is the critical support pressure of compressed air applied on free face. The fully support mode corresponds to the cases that H equals to D. As shown in Fig.1, k is the gradient of the support pressure, which can be expressed as $k=\tan\theta$. The support pressure is uniformly distributed when $\theta=0°$. The non-fully support mode cannot balance the external soil and water pressure completely. This would result in two serious problems in shield tunneling: surface settlement and face collapse failure. In this study, only the face stability problem will be discussed.

2.2 Solution of the critical support pressure

In this study, the rotational failure mechanism proposed by Mollon (2011) was used to determine the critical support pressure. This mechanism is consistent with the active failure mechanism observed in model tests (Kirsch 2010, Idinger *et al*. 2011). The spatial discretization technique was used to generate the rotational failure mechanism. As shown in Fig. 3, the shape of failure mechanism is determined by two parameters β_E and R_E/D. Point A, B are the intersections of crown and inverted arch with central axis. Point E is the center of tunnel face. The spiral body rotates around OX axis at a uniform angular velocity ω. The

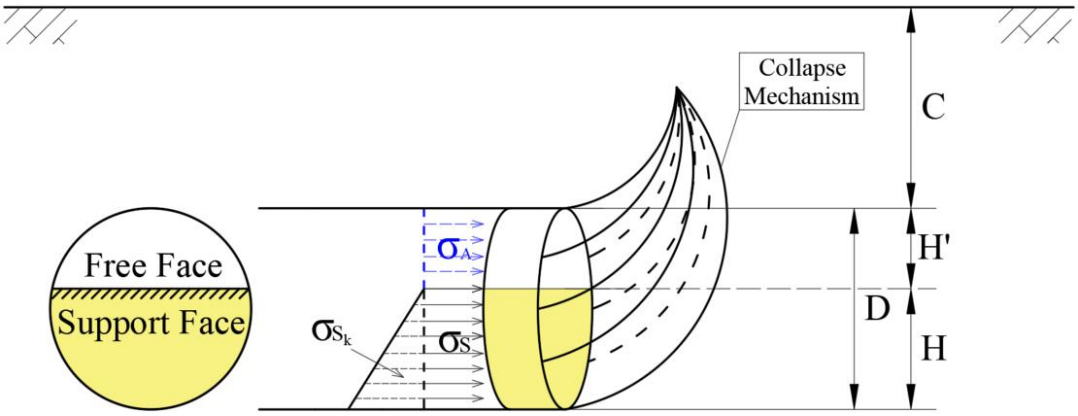

Fig. 2 Schematic diagram of non-fully support mode (σ_S: uniform support force, σ_{Sk}: gradient support force σ_A: compressed air support force)

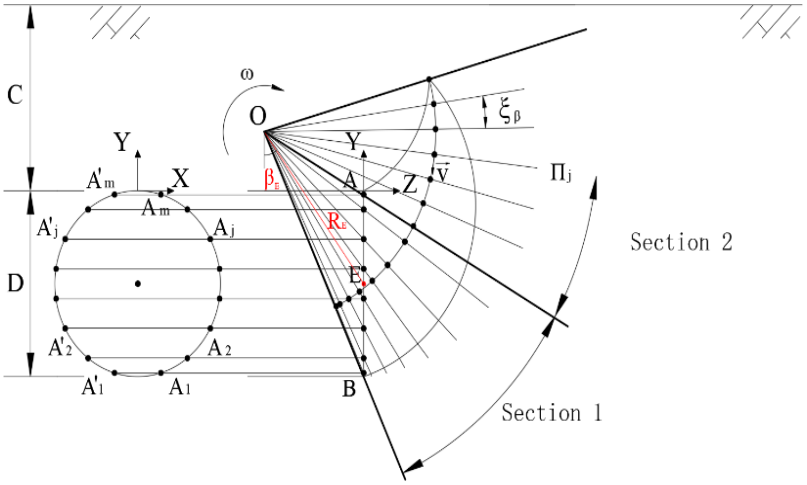

Fig. 3 Discretization technique for the collapse mechanism of tunnel face

velocity of any points in the failure mechanism is equal to the product of the angular velocity and the vertical distance from the point to the central axis of rotation.

Tunnel face is discretized by m groups of points symmetrical to the longitudinal axis. The helix is composed of two parts (Section 1 and 2, as shown in Fig. 3). The first section is discretized by a plurality of radial planes intersecting at the center O of polar coordinates and the normal lines are parallel to the velocity field. Section 2 is composed of the remaining radial planes. The contour points of the radial plane are all generated from the previous one. For instance, tunnel face consists of 2m points, A_1, A_2, ..., A_m. And the symmetric point is A_1', A_2', ..., A_m'. The intersection angle between radial planes is ξ_β. It is easy to understand that the discretization accuracy is determined by two parameters 'ξ_β' and 'm'. The calculation accuracy increases with the increase of two parameters, but the calculation time also increases at the same time. Refer to the cases in Mollons' study (2011), m and ξ_β are taken as 100 and 1.0°, respectively.

According to the upper bound theorem of limit analysis, Rate of internal energy dissipation W_D is less than or equal to the work rate of external force W_E is the necessary condition of the system to reach critically stabilized state. In this study, the work rate of external face W_E includes the work rate of effective gravity W_γ, supporting force $W_{\sigma T}$ and uniform surcharge acting on ground surface W_G if the failure mechanism outcrops. In this study, $W_{\sigma T}$ is comprised two parts: work rate of support force acting on support face $W\sigma_S$ and possible compressed air support force acting on free face $W\sigma_A$. According to Mollons' study (2011), the work rate of different external forces are as follows:

Work rate of support force of supporting medium

$$\begin{aligned}\dot{W}_{\sigma_S} &= \iint_S (\overrightarrow{\sigma_{Sk}} + \overrightarrow{\sigma_S}) \cdot \vec{v} d\Sigma \\ &= -\omega \cdot [k \cdot D \cdot \sum_{j=1}^{nm} (n - j/m) + \sigma_S] \\ &\cdot \sum_{j=1}^{nm} (S_j \cdot R_j \cdot \cos\beta_j)\end{aligned} \tag{1}$$

where σ_{sk} is the gradient support force acting on support face. σ_s is the uniform support force acting on support face. nD represents the height of support face. In this study, the specific gravity of supporting medium is adjusted by gradient k and the support area is changed by adjusting the summation upper bound nm. R_j and β_j are the polar coordinates of the point on support face. S_j represents the area of element at discretized face. ω is the angular

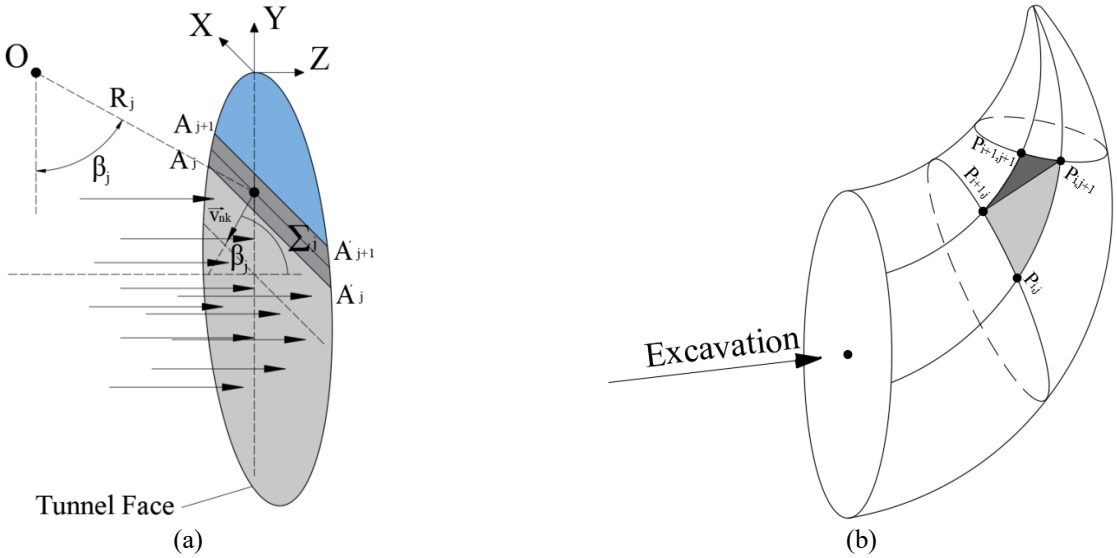

(a) (b)

Fig. 4 (a)Computation of the work rates of tunnel face and (b) Schematic of rotational failure mechanism

velocity of failure mechanism.

Work rate of compressed air support force acting on free face

$$\dot{W}_{\sigma_A} = \iint_S \overrightarrow{\sigma_A} \cdot \vec{v} d\Sigma = -\omega \cdot \sigma_A \cdot \sum_{j=nm+1}^{m-1} (S_j \cdot R_j \cdot \cos\beta_j) \tag{2}$$

where σ_A is the compressed air pressure acting on free face. For the cases of non-fully support mode with compressed air pressure, σ_A is uniformly distributed and equal to σ_s. In the analysis of non-fully support mode analysis, $\sigma_A = 0$.

Work Rate of possible uniform surcharge acting on ground surface (calculated when the failure mechanism outcrops)

$$\dot{W}_G = \iint_S \overrightarrow{\sigma_G} \cdot \vec{v} d\Sigma = \omega \cdot \sigma_G \cdot \sum_l (S_l \cdot R_l \cdot \sin\beta_l) \tag{3}$$

where σ_G is the ground surface surcharge. R_l and β_l are polar coordinates of the point on possible outcropping surface. S_l represents the area of element at outcropping surface. In this study, only active failure problem is discussed and W_G is ignored.

Work rate of effective gravity

$$\dot{W}_\gamma = \iiint_V \vec{\gamma} \cdot \vec{v} dV = \omega \cdot \gamma \cdot \sum_{i,j} (R_{i,j} \cdot V_{i,j} \cdot \sin\beta_{i,j} + R'_{i,j} \cdot V'_{i,j} \cdot \sin\beta'_{i,j}) \tag{4}$$

where $R_{i,j}$ and $\beta_{i,j}$ (respectively, $R'_{i,j}$ and $\beta'_{i,j}$) are the polar coordinates of the surface center of gravity of discrete micro tetrahedral elements in collapse mechanism. $V_{i,j}$ (respectively, $V'_{i,j}$) is the micro tetrahedral unit volume. γ is gravity of stratum soil.

In this study, internal energy dissipation only includes sliding resistance of soil W_C.

$$\dot{W}_C = \iint_S c \cdot v \cdot \cos\varphi \cdot dS = \omega \cdot c \cdot \cos\varphi \cdot \sum_{i,j} (S_{i,j} \cdot R_{i,j} + S'_{i,j} \cdot R'_{i,j}) \tag{5}$$

where c is cohesion of stratum soil. φ is the angle of internal friction. $S_{i,j}$ and $S'_{i,j}$ are the area of triangular faces $P_{i,j}P_{i+1,j}$ $P_{i,j+1}$ and $P_{i+1,j}P_{i,j+1}$ $P_{i+1,j+1}$..

Based on the upper bound theorem of limit analysis, by equating the work rate of internal energy loss and external force. The upper bound value of the limit support pressure can be derived as (Chen 1975)

$$\sigma_S = \gamma D N_\gamma - cN_c + \sigma_G N_G - kDN_k \tag{6}$$

The limit collapse support pressure can be obtained by maximize σ_s in equation (6). N_γ, N_c ,N_G and N_k are dimensionless coefficients. Four parameters are soil weight, cohesion, surface load and support modes impact factor respectively. The expressions are as follows

$$N_\gamma = \frac{\sum_{i,j} (R_{i,j} \cdot V_{i,j} \cdot \sin\beta_{i,j} + R'_{i,j} \cdot V'_{i,j} \cdot \sin\beta'_{i,j})}{D \cdot \sum_j (S_j \cdot R_j \cdot \cos\beta_j)} \tag{7}$$

$$N_C = \frac{\cos\varphi \cdot \sum_{i,j} (S_{i,j} \cdot R_{i,j} + S'_{i,j} \cdot R'_{i,j})}{\sum_j (S_j \cdot R_j \cdot \cos\beta_j)} \tag{8}$$

$$N_G = \frac{\sum_l (S_l \cdot R_l \cdot \sin\beta_l)}{\sum_j (S_j \cdot R_j \cdot \cos\beta_j)} \tag{9}$$

Table 1 Parameters of soil and segment

Material	Unit Weight /(kN·m^3)	Cohesion /(kPa)	Internal friction angle /(°)	Poisson's ratio	Elastic modulus /MPa
Stratum	18	7	20	0.3	24
Lining	25	-	-	0.2	1.5×10^4

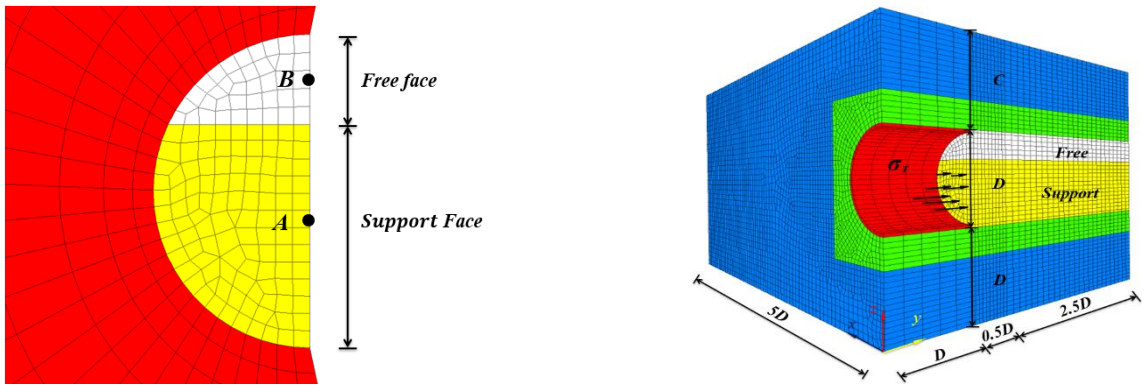

(a) (b)

Fig. 5 Non-fully support numercial model: (a) tunnel face and (b) integral model

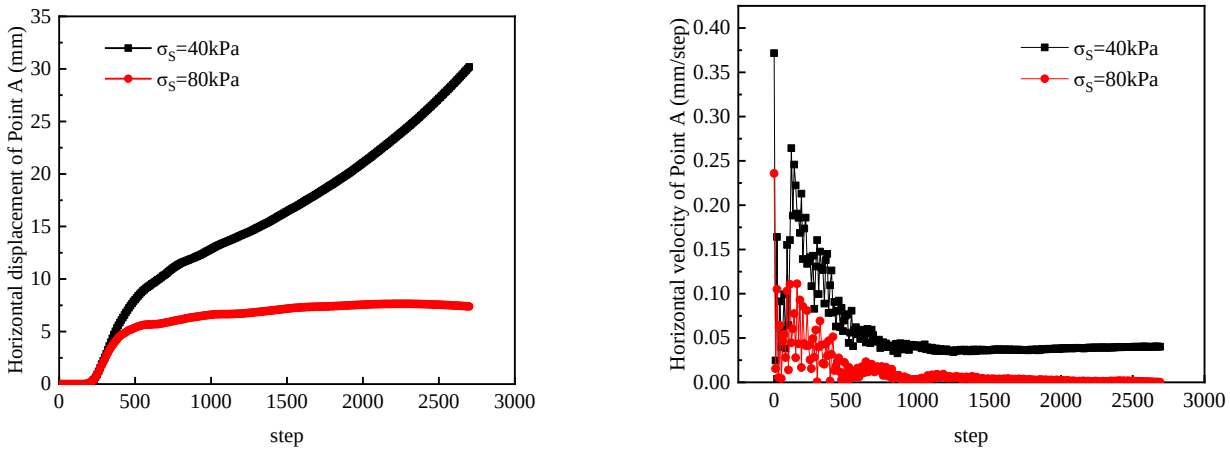

(a) (b)

Fig. 6 Variation of the horizontal displacement and the velocity of the tunnel face against the calculation steps: (a) Horizontal displacement and (b) Horizontal velocity

$$N_k = \frac{\sum_{j=1}^{nm}[(n-j/m)\cdot S_j \cdot R_j \cdot \cos\beta_j]}{\sum_j (S_j \cdot R_j \cdot \cos\beta_j)} \tag{10}$$

3. Comparisons

3.1 FLAC3D modelling

In order to verify the accuracy of proposed mechanism, numerical simulations of face failure under non-fully support mode were conducted by FLAC 3D. As shown in Fig. 5, both the tunnel diameter D and the cover depth C are 10 m. Segment lining thickness d is 0.3 m. In order to eliminate the boundary effect, the width of the model is set to 5D (Mollon *et al*. 2014). The three dimensions of the numerical model is 50 m×40 m×30 m (length×width×height, Fig. 5(b)). In order to increase the accuracy of the results, the mesh density around the tunnel face is enhanced locally.

The bottom of the model is constrained by fixed boundary, the surrounding is constrained by normal displacement, and the top is free boundary. Mohr-Coulomb constitutive model is adopted to simulate the soil and linear elastic model is adopted to simulate the segmental lining. The detailed parameters of soil and linings are listed in Table 1.

3.2 Determination of the face failure

In this study, the limit support pressure of tunnel face is determined by improved dichotomy method (Mollon *et al.* 2014). Compared with traditional stress control method, this method can reduce the calculation time required to reach

plastic flow state especially when the accuracy of the results is demanding. The improved dichotomy method is developed from the stress control method with higher computational efficiency, the basic steps are as follows: (i) Firstly, set the cohesion of soil to a very large value. This turns the soil into elastic material. (ii) Manually set the internal stress of the model to twice the initial value. Determine the step *N* required to return to equilibrium state of ground stress. By calculation, the value of *N* in this study is about 3900. (iii) Set the soil cohesion to initial value again. It is considered that the soil has entered the state of plastic flow if the model does not reach the equilibrium state after *N* calculation steps.

Choosing reasonable upper and lower limit value is the key to accurately calculate the critical support pressure. Fig. 6 shows the variation of horizontal displacement and velocity with calculation steps. The support ratio in this case is 0.7. The monitoring point was selected as the center of the support face. When σ_T=80 kPa, after 1500 calculation steps, the horizontal speed at point A has dropped to zero. While when σ_T=40 kPa, the horizontal displacement at point A continues to increase with a uniform rate after 2700 steps.

It indicates that when N is equal to 3900, it is reasonable to choose 80 kPa and 40 kPa as the upper and lower limit value.

3.3 Failure mechanism for different support modes

To verify the proposed model in this study, the numerical simulations were compared with the theoretical results. Fig. 7 shows the critical support pressure with different support ratios. The friction angle of the soil is 25°. The theoretical results show good agreement with the numerical simulations. For the conditions of support ratio is larger than 0.7, the difference between the theoretical calculations and numerical simulations is less than 5%.

However, when the support ratio is smaller than 0.7, the difference becomes larger. For the cases of n=0.3, the difference is 31.24%. It mainly because the local failure could occur at the unsupported face with the decrease of the support ratio. Specific analysis will be described in details in Section 4.2.

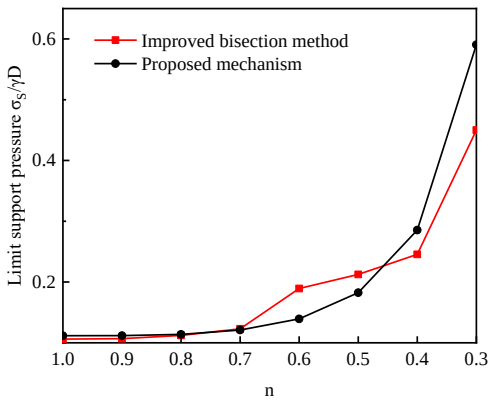

Fig. 7 Variation of the limit support pressure with the support ratios (k=0, c=7 kPa, φ=25°, C=D=10 m, γ=18 kN/m^3)

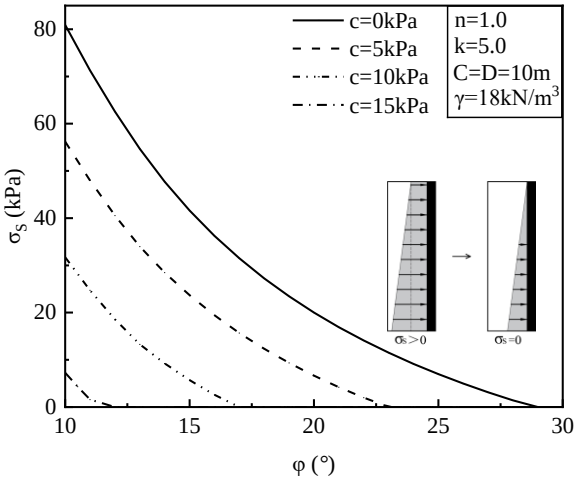

Fig. 8 Effect of stratum's internal frictional angle and cohesion on the critical support pressure σ_S

4. Parametric study

In the following analysis, the effect of the support modes as well as the tunnel diameter and geologic parameters on the critical support pressure are discussed. Elastic modulus and poisson ratio of the soil have almost no effect on the critical support pressure (Yu *et al*. 2020), so they are not considered in this study.

4.1 Fully support mode

Fig. 8 shows the effect of soil friction angle and cohesion on the critical support pressure. The friction angle φ ranges from 10° to 30° and the cohesion *c* ranges from 0 to 15 kPa. The pressure gradient is selected as 5.0 kPa/m. The critical support pressure σ_S corresponds to the pressure at the top of the tunnel face. It can be seen that the required support pressure gradually decreases with the increase of frictional angles. When σ_S decreases to 0, the support pressure mode changes from trapezoidal distribution to triangular distribution. Meanwhile, σ_S decreases with the increase of the soil cohesion, which indicates that the poorer the geologic conditions, the greater the support pressure required to maintain the stability of tunnel face.

Fig. 9 shows the effect of support pressure gradient on the critical support pressure. *k*=0 means that the support pressure is uniformly distributed on the tunnel face. It can be seen that the critical support pressure decreases linearly with the increase of k, which indicates that the assumption of uniform support pressure will overestimate the face stability. The face stability could be improved by increasing the specific gravity of the support medium, e.g., slurry, soil muck etc. For instance, engineers can use a high density slurry to improve the face stability.

With the increasing demand for transportation infrastructure, the diameter of tunnels is becoming larger and larger. Some tunnels built by shield machines are even close to 20 m nowadays. In this study, the effect of the tunnel diameter on the critical support pressure under the fully support mode condition is discussed. The range of the

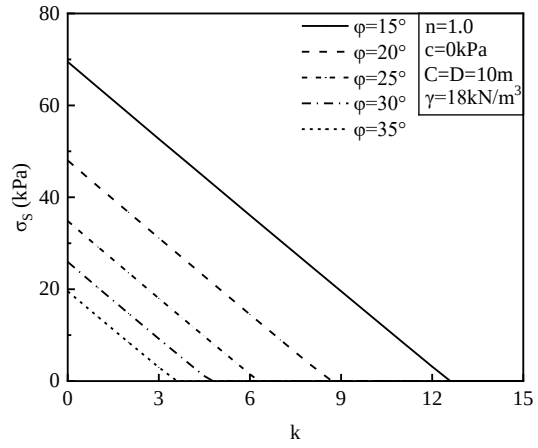

Fig. 9 Effect of the support pressure gradient k on the critical support pressure σ_S

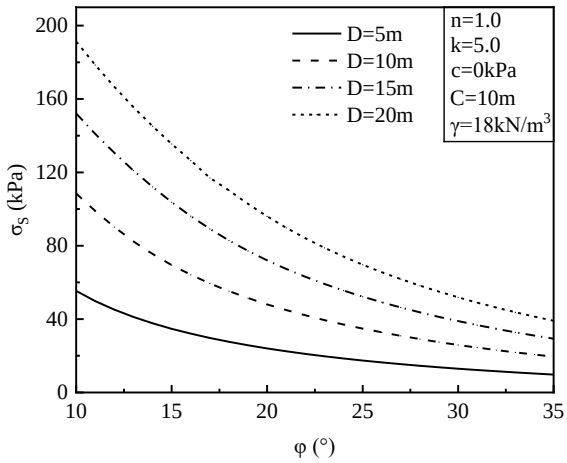

Fig. 10 Effect of the tunnel diameter on critical support pressure σ_S

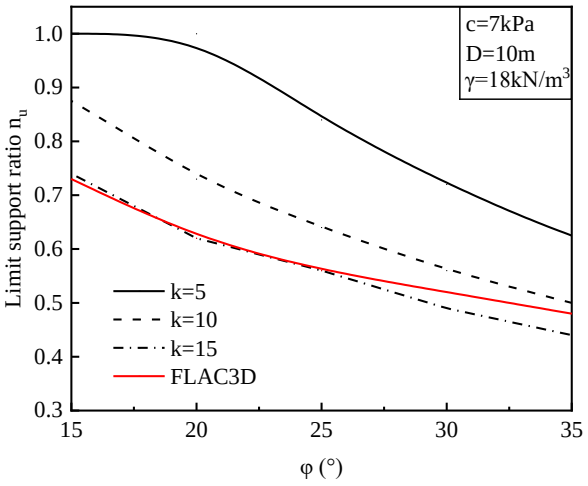

(a)

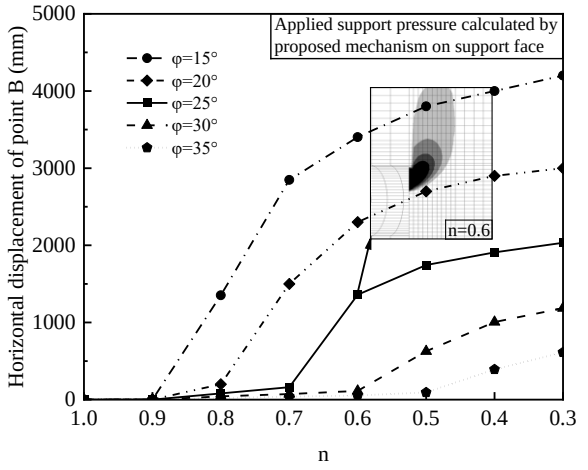

(b)

Fig. 11 Global failure and local failure of tunnel face (a) Limit support ratios for face failure and (b) Local failure under different soil frictional angles

tunnel diameters is selected between 5-20m in this study. As shown in Fig. 10, the required support pressure gradually increases with the increase of the tunnel diameter, indicating that the larger the tunnel diameter, the greater the risk of tunnel collapse. This is because there is a pressure difference between the support pressure in the excavation chamber and the external soil pressure, and the pressure difference will increase with the increase of tunnel diameter.

4.2 Non-fully support mode

Although it is desirable to use the non-full support mode to increase the advance ratio or replace cutting tools, ground collapse is also prone to occur in this mode. In this study, the allowed support ratio n_u is investigated through the proposed model. The effect of soil friction angle on the limit support ratio is shown in Fig. 11(a). The pressure gradient k ranges from 5.0-15.0. It can be seen that the allowed support ratio gradually decreases with the increase of soil friction angle. It shows that the higher the soil strength, the smaller the area of the support face required. The lower the support pressure gradient is, the larger the area of the support face required. Engineers should carefully determine the allowed support ratio before adopting the non-fully support mode.

However, when the support ratio continually decreases, the local failure at the free face could be found. The local failure means the soil at the free face collapse locally. Once the local failure occurs, the magnitude of the support pressure and the support height are meaningless for the face stability. The local failure of the tunnel face is obtained by FLAC 3D. Fig. 11(b) shows the variation of horizontal displacement at the unsupported face with the support ratio. The monitoring point is located at the center of the free face. It could be found that the displacement suddenly gets larger with the decrease of the support ratios, which indicates the local failure at the free face occurs at this support ratio. The larger the friction angles, the smaller the support ratios. According to the velocity maps in Fig. 11(b), global failure of the tunnel face occurs when n decreases to 0.6 for the cases of φ=25°. Different from the global failure, in the local failure, only the soil close to the unsupported part of the tunnel face will collapse. Thereafter, increasing the pressure of the supporting face cannot help to maintain the stability of the tunnel face. Because the local failure

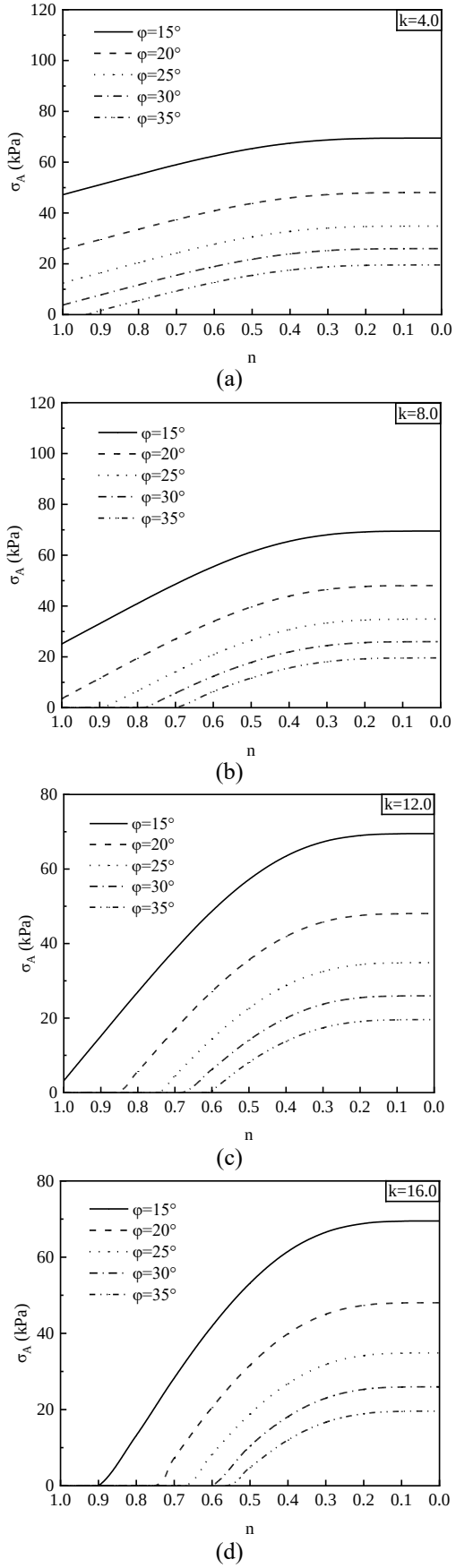

Fig. 12 Relationship between critical compressed air pressure σ_A with different support ratio and pressure gradient (a) k=4.0, (b) k=8.0, (c) k=12.0 and (d) k=16.0

would expand to ground surface and become to global failure. The limit support ratios corresponding to the local failure are also plotted in Fig. 11(a). The pressure gradient k has almost no effect on the local failure, this is reasonable because the local failure mainly depends on the unsupported area. It indicates that for the case of k=15 kPa/m, local failure has appeared before the global failure. In order to avoid local failure of the tunnel face, compressed air pressure usually should be supplemented to conduct the non-fully support modes.

To avoid of the local failure in non-fully support mode, compressed air is usually used to provide compensatory pressure to keep face stability. Fig. 12 provides the design charts of the required air pressure for face stability. n=1.0 means that the chamber is filled with supporting medium, while n=0.0 means the chamber is filled with compressed air. It can be seen that the air pressure σ_A increases gradually with the decrease of support ratios, while it decreases with the increase of soil friction angle φ. Additionally, the air pressure first increases rapidly with the decrease of support ratio, then, it trend toward a stable value when the support ratio is less than 0.3. Take φ=15°, k=4.0 as an example, when n decreases from 1.0 to 0.3, the air pressure σ_A increases by 45.7%. When n decreases from 0.3 to 0, the air pressure σ_A only increases by 1.0%. This indicates that tunnel face stability is mainly maintained by compressed air support pressure under a low support ratio. Moreover, the required air pressure σ_A gradually decreases with the increases of the pressure gradient k under the same support ratio. It means that increasing the specific gravity of supporting medium is helpful to improve the stability of tunnel face even under the non-fully support mode. The use of the compressed air has the following advantages: contributing to the face stability, improving the excavation efficiency and providing space for equipment maintenance.

5. Conclusions

This paper studied the failure mechanism of tunnel face under the non-fully support mode. The proposed method could be used for the evaluation of the ground collapse and determine the compressed air pressure required for face stability maintenance. The main work of this paper is summarized as follows:

- The support pressure gradient has significant effect on the stability of tunnel face under poor geology conditions. Increasing the specific gravity of supporting medium could contribute to the stability of tunnel face, while the increase of tunnel diameter could be unfavorable for the face stability. The assumption of uniform support pressure on tunnel face would underestimate the failure risk.
- Local failure may occur before global failure for the cases of non-fully support mode when the soil is very poor. The critical support ratio is used to evaluate the face stability under the non-fully support mode, which could be an important index to determine whether the specific unsupported height could be allowed during shield tunneling.

- To avoid of the local failure in non-fully support mode, compressed air is usually used to provide compensatory pressure to keep face stability. The required air pressure increases gradually with the decrease of support ratios. Several charts are provided for the assessment of compressed air pressure, which could help engineers to determine the required air pressure for face stability.

This study does not consider the seepage failure that may occur in water-rich ground. More analysis should be carried out in further studies.

Acknowledgments

The authors gratefully acknowledge the financial support from the Fundamental Research Funds for the Central Universities under Grant No. 2021RC231 and the National Natural Science Foundation of China under Grant No. 52008021.

References

Chen, R.P., Li, J., Kong, L.G. and Tang, L.J. (2013), "Experimental study on face instability of shield tunnel in sand", *Tunn. Undergr. Sp. Tech.*, **33**, 12-21. https://doi.org/10.1016/j.tust.2012.08.001.

Chen, R., Yin, X., Tang, L. and Chen, Y. (2018), "Centrifugal model tests on face failure of earth pressure balance shield induced by steady state seepage in saturated sandy silt ground", *Tunn. Undergr. Sp. Tech.*, **81**, 315-325. https://doi.org/10.1016/j.tust.2018.06.031.

Chen, W.F. (1975), Limit analysis and soil plasticity, Elsevier, Amsterdam.

Eberhardt, E. (2001), "Numerical modelling of three-dimension stress rotation ahead of an advancing tunnel face", *Int. J. Rock Mech. Min. Sci.*, **38**(4), 499-518. https://doi.org/10.1016/S1365-1609(01)00017-X.

Idinger, G., Aklik, P., Wu, W. and Borja, R.I. (2011), "Centrifuge model test on the face stability of shallow tunnel", *Acta Geotechnica*, **6**(2), 105-117. https://doi.org/10.1007/s11440-011-0139-2.

Jin, D., Zhang, Z. and Yuan, D. (2021), "Effect of dynamic cutterhead on face stability in epb shield tunneling", *Tunn. Undergr. Sp. Tech.*, **110**(1), 103827. https://doi.org/10.1016/j.tust.2021.103827.

Ji, X., Ni, P., Barla, M., Zhao, W. and Mei, G. (2018), "Earth pressure on shield excavation face for pipe jacking considering arching effect", *Tunn. Undergr. Sp. Tech.*, **72**, 17-27. https://doi.org/10.1016/j.tust.2017.11.010.

Juneja, A., Hegde, A., Lee, F.H. and Yeo, C.H. (2010), "Centrifuge modelling of tunnel face reinforcement using forepoling", *Tunn. Undergr. Sp. Tech.*, **25**(4), 377-381. https://doi.org/10.1016/j.tust.2010.01.013.

Kirsch, A. (2010), "Experimental investigation of the face stability of shallow tunnels in sand", *Acta Geotechnica*, **5**(1), 43-62. https://doi.org/10.1007/s11440-010-0110-7.

Li, P., Chen, K., Wang, F. and Li, Z. (2019), "An upper-bound analytical model of blow-out for a shallow tunnel in sand considering the partial failure within the face", *Tunn. Undergr. Sp. Tech.*, **91**, 102989. 1-102989.12. https://doi.org/10.1016/j.tust.2019.05.019.

Lu, P., Yuan, D., Chen, J., Jin, D., Wu, J. and Luo, W. (2021), "Face stability analysis of slurry shield tunnels in rock-soil interface mixed ground", *KSCE J. Civil Eng.*, **25**(6), 2250-2260. https://doi.org/10.1007/s12205-021-1254-8.

Liu, W., Zhao, Y., Shi, P., Li, J. and Gan, P. (2018), "Face stability analysis of shield-driven tunnels shallowly buried in dry sand using 1-g large-scale model tests", *Acta Geotechnica*, **13**(3), 693-705. https://doi.org/10.1007/s11440-017-0607-4.

Liu, X.Y., Fang, H.Y., Wang, F.M. and Yuan, D.J. (2021), "Horizontal trap-door investigation on face failure zone of shield tunneling in sands", *J. Central South Univ.*, **28**(3), 866-881. https://doi.org/ 10.1007/S11771-021-4632-Y.

Mollon, G., Dias, D. and Soubra, A.H. (2009), "Probabilistic analysis of circular tunnels in homogeneous soil using response surface methodology", *J. Geotech. Geoenviron. Eng.*, **135**(9), 1314-1325. https://doi.org/10.1061/(ASCE)GT.1943-5606.0000060.

Mollon, G., Dias, D. and Soubra, A.H. (2011), "Rotational failure mechanisms for the face stability analysis of tunnels driven by a pressurized shield", *Int. J. Numer. Anal. Method. Geomech.*, **35**(12), 1363-1388. https://doi.org/10.1002/nag.962.

Nagel, F. and Meschke, G. (2010), "An elasto-plastic three phase model for partially saturated soil for the finite element simulation of compressed air support in tunneling", *Int. J. Numer. Anal. Method. Geomech.*, **34**(6), 605-625. https://doi.org/10.1002/nag.828.

Paternesi, A., Schweiger, H.F. and Scarpelli, G. (2017), "Numerical analyses of stability and deformation behavior of reinforced and unreinforced tunnel faces", *Comput. Geotech.*, **88**, 256-266. https://doi.org/10.1016/j.compgeo.2017.04.002.

Pan, Q. and Dias, D. (2016), "The effect of pore water pressure on tunnel face stability", *Int. J. Numer. Anal. Method. Geomech.*, **40**(15), 2123-2136. https://doi.org/10.1002/nag.2528.

Perazzelli, P., Leone, T. and Anagnostou, G. (2014), "Tunnel face stability under seepage flow conditions", *Tunn. Undergr. Sp. Tech.*, **43**, 459-469. https://doi.org/10.1016/j.tust.2014.03.001.

Qarmout, M., König, D., Gussmann, P., Thewes, M. and Schanz, T. (2019), "Tunnel face stability analysis using Kinematical Element Method", *Tunn. Undergr. Sp. Tech.*, **85**, 354-367. https://doi.org/10.1016/j.tust.2018.11.024.

Subrin, D. and Wong, H. (2002), "Tunnel face stability in frictional material: a new 3D failure mechanism", *Comptes Rendus Mecanique*, **330**(7), 513-519. https://doi.org/10.1016/S1631-0721(02)01491-2.

Sterpi, D. and Cividini, A. (2004), "A physical and numerical investigation on the stability of shallow tunnels in strain softening media", *Rock Mech. Rock Eng.*, **37**(4), 277-298. https://doi.org/10.1007/s00603-003-0021-0.

Tang, X.W., Liu, W., Albers, B. and Savidis, S. (2014), "Upper bound analysis of tunnel face stability in layered soils", *Acta Geotechnica*, **9**(4), 661-671. https://doi.org/10.1007/s11440-013-0256-1.

Tian, Y., Du, S., Sun, W. and Cheng, K. (2019), "Study on tunneling parameters and surface subsidence of large-diameter slurry shield based on half-chamber air pressure method", *J. Railway Sci. Eng.*, **16**(10), 2530-2537. https://doi.org/10.19713/j.cnki.43-1423/u.2019.10.020.

Wang, T., Yuan, D., Jin, D. and Li, X. (2021), "Experimental study on slurry-induced fracturing during shield tunneling", *Front. Struct. Civil Eng.,* **15**(2), 333-345. https://doi.org/10.1007/s11709-021-0718-8.

Wang, H., Huang, M., Lv, X. and Zhou, W. (2013), "Upper-bound limit analysis of stability of shield tunnel face considering seepage", *Chinese J. Geotech. Eng.*, **35**(4), 1696-1704. https://doi.org/CNKI:SUN:YTGC.0.2013-09-020.

Yang, X.L. and Huang, F. (2011), "Collapse mechanism of shallow tunnel based on nonlinear Hoek–Brown failure criterion", *Tunn.*

Undergr. Sp. Tech., **26**(6), 686-691. https://doi.org/10.1016/j.tust.2011.05.008.

Yuan, D., Shen, X., Liu, X. and Wu, J. (2017), "Research on excavation face stability of slurry shield tunneling", *China J. Highway Transport*, **30**(8), 24-37. https://doi.org/10.3969/j.issn.1001-7372.2017.08.003.

Yu, L., Zhang, D., Fang, Q., Cao, L., Zhang, Y. and Xu, T. (2020), "Face stability of shallow tunnelling in sandy soil considering unsupported length", *Tunn. Undergr. Sp. Tech.*, **102**, 103445. https://doi.org/10.1016/j.tust.2020.103445.

Zhang, Z.X., Hu, X.Y. and Scott, K.D. (2011), "A discrete numerical approach for modeling face stability in slurry shield tunnelling in soft soils", *Comput. Geotech.*, **38**(1), 94-104. https://doi.org/10.1016/j.compgeo.2010.10.011.

Zhang, Z., Huang, M., Zhang, C., Jiang, K. and Bai, Q. (2020), "Analytical prediction of tunneling-induced ground movements and liner deformation in saturated soils considering influences of shield air pressure", *Appl. Math. Model.*, **78**, 749-772. https://doi.org/10.1016/j.apm.2019.10.025.

Zhu, W.B. and Ju, S.J. (2006), Shield tunneling technology in mixed face ground conditions, China science and technology press, Beijing.

Zhu, W., Qian, Y., Wang, L., Hu, J., Xing, H. and Lu, K. (2020), "Problems and measures of earth pressure balance shield during construction with the unfilled chamber", *China J. Highway Transport*, **33**(12), 224-234. https://doi.org/10.1016/10.19721/j.cnki.1001-7372.2020.12.018.

Zou, J., Chen, G. and Qian, Z. (2019), "Tunnel face stability in cohesion-frictional soils considering the soil arching effect by improved failure models", *Comput. Geotech.*, **106**, 1-17. https://doi.org/10.1016/j.compgeo.2018.10.014.

CC